Available online at www.sciencedirect.com
ScienceDirect
Journal of Photochemistry and Photobiology A: Chemistry 182 (2006) 310–318
Journal of Photochemistry and Photobiology A:Chemistry
www.elsevier.com/locate/jphotochem

Selective activation of material property changes in photostructurable glass ceramic materials by laser photophysical excitation

Frank E. Livingston, Henry Helvajian *

Micro/Nanotechnology Department, Space Materials Laboratory, The Aerospace Corporation, Los Angeles, CA 90009, United States

Available online 21 July 2006

Abstract

We propose a novel approach to material processing: one that implements laser photoexcitation in a direct-write scheme to establish initial excitation states in a protean material that enables the regulation of a particular phase transformation pathway. The effect of regulating the phase transformation process is the controlled alteration of a specific material property. As a test of the concept, we have investigated a class of photostructurable glass ceramics (PSGCs) of the lithium aluminosilicate family. By controlling the incident laser irradiance (i.e., the material exposure), we can affect the material solubility, optical transmission, and material hardness following the phase transformation process. To further enhance the fidelity of the laser photo-induced reaction process, we have developed a scheme that permits the controlled delivery of laser photons during complex motion patterning maneuvers.
© 2006 Published by Elsevier B.V.

Keywords: Photochemistry and photophysics of laser processing; 3D microfabrication; Photolytic control of material properties of photostructurable glass ceramics; Variable dose direct-write patterning

1. Introduction

Since their invention nearly 60 years ago, glass ceramic materials have been used in a wide range of applications from human health (e.g., medical and dental) to consumer commodities (e.g., electronics) to transportation (e.g., aerospace) [1]. The technological appeal of this material class is that it is manufactured in the glassy amorphous phase, shaped if necessary via low cost "plastic" molding techniques, and then converted via a heat treatment step to the final ceramic form. The ceramization or crystallization process is typically a sequential two-step process that is initiated by the formation of a precipitate or nucleating species. Although the nucleation and ceramization can be viewed as a two-step process, the near sequential processes relegate it as a single step that is primarily governed by temperature. The photostructurable glass ceramics (PSGCs) are a subclass of the general class of glass ceramics. These materials include additives that separate the nucleation and crystallization (i.e., ceramization) processes into two distinct steps. This is accomplished by addition of photo-sensitizer compounds that initiate the nucleation step. The advantage of the PSGC materials compared with common glass ceramics is that the ceramization process need not be global. Lithographic techniques can be used for patterning and the exposed areas can be subsequently converted into at least two distinct ceramic phases, one of which is soluble in dilute hydrofluoric (HF) acid. The consequence is the ability to fabricate intricate microstructures in glass ceramic materials by either mask-lithography or laser direct-write patterning techniques [2]. However, beyond fabricating microstructure shapes it may be possible to also locally alter the material properties to make it more amenable for the application. In the PSGCs, the material phase transformation process is photolytically initiated. Since the material undergoing the phase transformation process is likely to exhibit a change in the material properties, it becomes possible to acquire some measure of control over the extent to which these material property changes are exhibited by controlling the initial sensitization process. A new processing capability can be derived based on the fact that new material properties or changes in material properties can be "turned on" a local scale by patterning and photoexcitation. In a recent series of experiments, we have explored the effect of controlling the laser irradiation exposure (dose) and the subsequent thermal processing protocol on three material properties for the commercially available PSGC Foturan™. The material properties investigated include the optical transmission, the solubility in dilute acid, and the mechanical strength [3]. The objective for

* Corresponding author. Tel.: +1 310 336 7621; fax: +1 310 563 3175.
E-mail address: henry.helvajian@aero.org (H. Helvajian).

1010-6030/$ – see front matter © 2006 Published by Elsevier B.V.
doi:10.1016/j.jphotochem.2006.04.044

these investigations corresponds to the ability to locally alter specific properties, which can be utilized in the development of glass ceramic microsystems [4].

In this publication, we present experimental results that support the notional idea that controlling the photoexcitation source can result in practical advantages when applied to a certain class of photofunctional materials. In this case, the photofunctional material is the glass ceramic and the advantages that are gained facilitate the fabrication of true three-dimensional (3D) micro engineered structures and the development of integrated devices. Our results demonstrate that the material solubility can be "turned on" a local scale by controlling the laser irradiance. The outcome is a material processing technique that enables the co-fabrication of complex microstructures without requiring masking layers for either patterning or protection during chemical etching. We show additional experimental evidence that other material properties can be similarly controlled on a local scale. Our results for the PSGCs suggest that it should be possible to develop a unique class of photofunctional glass ceramic materials whereby the initial photoexcitation event establishes the conditions that dictate the pathway to reaching a particular "final state" that has the desired functional property.

2. Photostructurable glass ceramics

The extent to which a photolytically driven process can controllably be executed normally depends on the degree of control that can be exercised during the photolysis step, the characterization detail of the material under investigation and on the level of fundamental understanding with regards to the pertinent photochemical and photophysical processes. In our laboratory, we have focused on elucidating the pertinent photochemical and photophysical processes, but recognize that because we lack control of the material development of the commercial Foturan product, our level of understanding cannot yet breach the specific photophysical/chemical reaction pathways. As a consequence, our goal has been to explore the main processes that are thought to be operative in the general class of PSGC materials.

In most commercially available PSGC materials, the photoinitiation and the subsequent "fixing" of the exposure processes proceed via three generalized equations as shown below [5]. The equations are written for the particular constituents found in Foturan but are representative of the processes in PSGCs. Eq. (1) describes the photoexcitation process that generates an electron in a trapped state. For the photoelectron donor species, cerium, the absorption peak is located in the ultraviolet (UV) region near 315 nm. Eq. (2) describes the thermophysical process that reduces nascent silver ions, and Eq. (3) describes the formation of a silver cluster or "precipitate", which characterizes the "fixing" of the exposure. The "fixing" process occurs at low temperatures (~450–500 °C) and marks the beginning of the heterogeneous nucleation phase and the growth of various possible crystalline phases. In the case of the PSGC Foturan, manufactured by the Schott Corporation, a lithium metasilicate (Li_2SiO_3) crystalline phase grows at temperatures near 600 °C and a lithium disilicate ($Li_2Si_2O_5$) crystalline phase is observed at higher temperatures (~700–800 °C). The Li_2SiO_3 metasilicate phase is soluble in HF while the disilicate $Li_2Si_2O_5$ is comparatively inert [6].

$$Ce^{3+} + h\nu \rightarrow Ce^{4+} + e^- \quad (1)$$

$$Ag^+ + e^- \xrightarrow{\Delta H} Ag^0 \quad (2)$$

$$xAg^0 \xrightarrow{\Delta H} (Ag^0)_x \quad (3)$$

Simple analysis reveals that the chemical etching rate of the lithium metasilicate ceramic phase should depend on the number of incident photons ($I/h\nu$), where I is the laser irradiance (W/cm^2) and $h\nu$ is the energy per photon. The logic follows the set of equations as presented below. We first assume that the etch rate ($R_{crystal}$) of a thermally processed glass ceramic to form the lithium metasilicate phase is proportional to the concentration of [Li_2SiO_3] crystals (Eq. (4)). However, the concentration of [Li_2SiO_3] should be proportional to the silver cluster density (Eq. (5)), $(Ag^0)_x$, since it is the silver clusters that induce the precipitation of the metasilicate phase. The cluster density is related to the concentration of reduced silver atoms, Ag^0, which can be related to the number of photo excited electrons (e^-) that are involved in the silver ion redox process (Eqs. (1)–(3) and (6)). Finally, the chemical etching rate is related to the number of incident photons (Eq. (7)) by association.

$$R_{crystal} \propto [Li_2SiO_3] \quad (4)$$

$$[Li_2SiO_3] \propto [Ag_x{}^0] \quad (5)$$

$$[Ag_x^0] \propto [Ag^0] \propto [e^-] \propto \left[\frac{I}{h\nu}\right] \quad (6)$$

$$R_{crystal} \propto \left[\frac{I}{h\nu}\right] \quad (7)$$

3. Results

3.1. Effect of laser irradiance on phase transformed material state properties

To demonstrate the correlation between the chemical etching rate and incident photon irradiance, an experiment was conducted to expose glass samples with a high degree of accuracy. The exposure tool was a pulsed laser operating at $\lambda = 355$ nm. Fig. 1 shows the results of these experiments, where the etch depth is plotted as a function of etch time for a set of laser irradiance values. The change in the slope for the fitted data supports the notion that the chemical etching rate is dependent on the laser irradiance.

The data in Fig. 1 can be recast in a more practical form as the etch contrast or etch ratio. This parameter represents the ratio of the etch rate of the exposed material divided by the etch rate of the unexposed but yet thermally processed material. The etch ratio or contrast is the parameter that is desired for material processing as it defines the maximum aspect ratio that can be achieved for a patterned structure in Foturan PSGC. In a complementary series of experiments, the etch rate of the native glass was measured following thermal processing and determined to

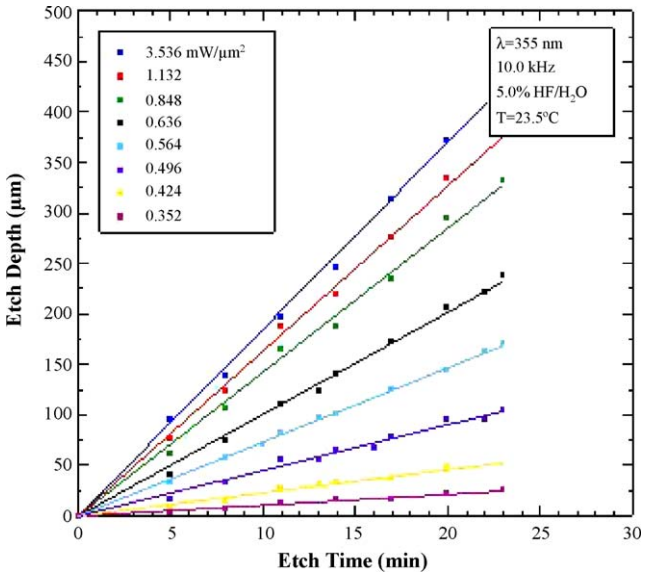

Fig. 1. Measured etch depth as a function of etch time for laser-irradiated and thermally-processed Foturan at λ = 355 nm.

be 0.62 + 0.06 μm/min. Fig. 2 shows the data of Fig. 1 recast in terms of the etch ratio or contrast and plotted as a function of laser irradiance. Fig. 2 also shows a companion data set for laser exposures measured using excitation at λ = 266 nm [7]. Recast in this format, the data exhibit a number of interesting features. First, the etch rate ratio appears to saturate at a value near 30:1 regardless of the exposure wavelength. These results suggest that the phase transformation process that results in the etchable Li_2SiO_3 crystalline phase does not critically depend on differences in the trapped electron states accessed by the different wavelengths. The etch rate ratio has a stronger correlation with the thermal processing profile. Second, much less laser irradiance is required to achieve contrast saturation for λ = 266 nm exposure compared with λ = 355 nm exposure. These results argue that even though the solubility of the etchable phase (i.e., material final state) is not dependent on the laser exposure wavelength, the reaction kinetics that drive the formation of the crystalline phase is dependent on the laser wavelength. Third, prior to reaching the condition of etch contrast saturation, the data show that there is a region of laser irradiances in which the etch rate ratio is a monotonically increasing function and can be linearized to define a slope. Furthermore, the defined slope for λ = 355 nm is approximately 10 times smaller compared with the slope for λ = 266 nm. The fact that there is a region of laser irradiances where the etch contrast can be linearized suggests that it may be possible to controllably vary the etch rate ratio and thereby gain some modicum of precision. Finally, the large difference between the two data fit slopes suggests that the distribution of reagents generated by 266 nm laser irradiation is more efficient in forming the metasilicate species (i.e., Li_2SiO_3).

The general conclusions that can be derived are that both the laser wavelength and the irradiance can be used to set an appropriate set of exposure conditions that affect a final phase transformed material state. In this case, the controlled property corresponds to the etch rate or the effective solubility of the material. The results of Fig. 2 also suggest that it may be possible to control the mechanical properties of the material, although it is to a more limited extent. The published values of the Young's modulus are 78 GPa for the unexposed glass and nearly 88 GPa for the region where the etch ratio is saturated [8]. The modulus of rupture over the same range varies from 60 to 150 MPa [8]. Using X-ray diffraction (XRD) spectroscopy, we have measured the extent of crystallinity as a function of laser irradiance and the data shows a dependence mimicking the data presented in Fig. 2 [9]. We are also now initiating experiments to exploit the ability to locally control the mechanical properties of Foturan for the development of complex microsystems.

The results presented in Fig. 2 conceal another conclusion, one that is technological in nature and concerns how the data was acquired. To accurately measure the etch rate properties within a narrow processing window of laser irradiances (e.g., λ = 266 nm) requires a laser with stable output power. The significance is that it is now technologically possible to control pulsed laser irradiances to a level of precision that was not achievable 8 years ago. To accurately measure the data presented in Fig. 2, the fluctuations of the incident laser average power had to be kept

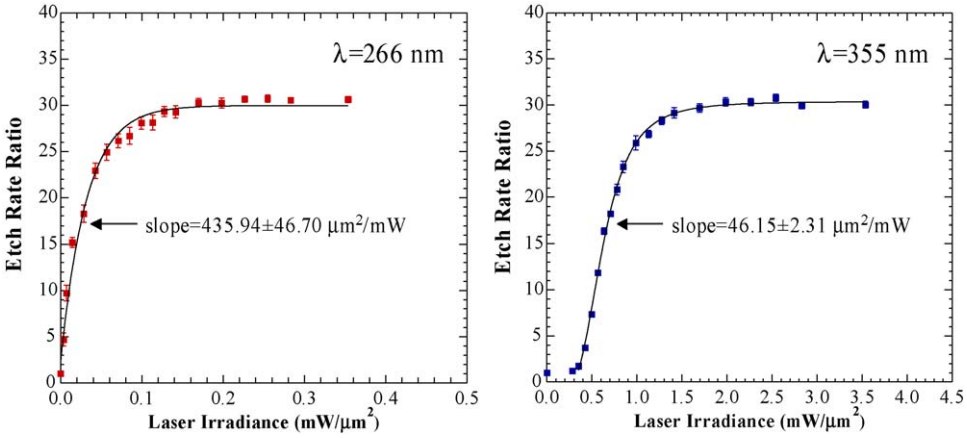

Fig. 2. Measured etch rate ratios as a function of incident laser irradiance at λ = 266 nm (left) and 355 nm (right). The solid squares correspond to the measured etch rate results and the solid lines represent optimized Hill equation fits to the experimental data.

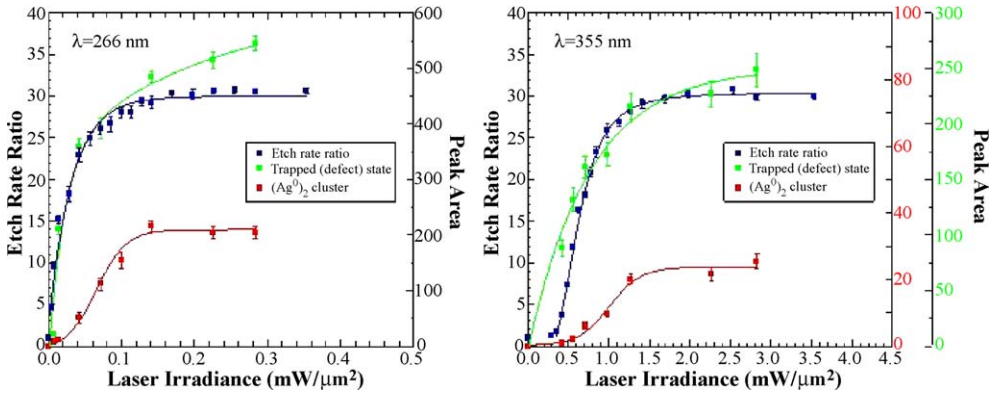

Fig. 3. Comparison of the photophysical measurements (peak area; right axis) and the chemical etching data (etch rate ratio; left axis) for laser exposure processing at λ = 266 nm (left) and 355 nm (right).

to a fraction of a mW over a 6 h period. Furthermore, it was also necessary to have a commanded resolution approaching tens of μWs for laser power selection. The fact that it is now possible to maintain this level of power stability is a consequence of the development of diode-pumped solid-state lasers and the more recently advances made in fiber laser technology. In both systems the power drift issues have been largely solved. This revolution in laser technology makes it possible to confidently conduct experiments in precision laser exposure. Furthermore, it allows for investigations on the use of photoexcitation to alter concentrations of intermediate state "reagents" and observe the effect on a final state phase-transformed material property.

In Fig. 3, we present additional data on the concentration of two intermediate state "reagents" measured as a function of laser irradiance for two common solid-state laser wavelengths (λ = 266 and 355 nm). These "reagent" species characterize two intermediate states of the PSGC material while undergoing thermal processing. Plotted along with the etch rate ratio data of Fig. 2 is the concentration of the initial photo-generated electrons (Eq. (1)) and the concentration of silver clusters produced by the redox process (Eq. (3)). Both data were measured via optical absorption spectroscopy [10]. The photo-generated electron is identified in the plot as the trapped defect state and is characterized by an absorption band at 265–280 nm. The measurement of the silver cluster species has a characteristic spectroscopic signature at 420 nm [11]. The results from both wavelength exposures are directly comparable since all the absorption data has been reduced to integrated linear absorption coefficients and identified in the plot in units of peak area. The results show that both the photoelectron defect state concentration and the silver cluster concentration follow the etch rate ratio curve as it bends toward saturation. Keeping in mind the sequence of events in the reaction process, the photoelectrons are generated at room temperature and this is followed by the formation of silver clusters at elevated temperatures (450–500 °C). The data show that the silver cluster concentration saturates with increasing laser irradiance, but within our error bars, there appears to be no similar saturation behavior for the photoelectron defect state concentration. The photoelectron concentration does not appear to have been fully titrated in the silver redox process. Further review of the data show that the concentrations of the photoelectron defects and silver clusters (identified by peak area units) are larger for laser irradiation at 266 nm compared with laser irradiation at 355 nm. This composite data provides insight into the thermal reaction kinetics that drive the formation of the crystalline Li_2SiO_3 material state and offers the opportunity to explore the effects on the final state properties by altering the critical kinetic processes through controlled photoexcitation. For example, it is known that the precipitation of the Li_2SiO_3 phase requires a minimum cluster size of ∼8 nm. Perhaps it is possible to alter the Ag_x cluster size distribution by direct absorption of laser light within the 420 nm plasmon band [12] and observe the effects on the nucleation kinetics. These experiments are currently underway in our laboratory.

Regardless of whether the photoexcitation of the intermediate state "reagents" can exert appreciable influence on other final state material properties, it is clear from the data of Figs. 2 and 3 that by the mere imposition of controlling the laser irradiance it is possible to influence both the kinetics and a final state property. Fig. 4 presents the controlled change of the PSGC transmission in the infrared (IR) region. The data shows measurements of the optical transmission as a function of the incident laser irradiance at λ = 355 nm. The data on the left present the measured transmission spectra, while the data on the right show how the average transmission near the 1.7 μm wavelength region changes with the initial exposure irradiance. The results indicate that it should be possible to control the material IR transmission by at least a factor of two to three by direct control of the incident laser power.

Additional control of the absorption in the UV region is also possible. In Foturan PSGC, the Ce^{3+} chromophore has a $4f^1$ electronic configuration and therefore a $^2F_{5/2}$ ground state. The only f–f transition is to the $J = 7/2$ electronic state and this occurs in the infrared (∼0.248 eV) [13]. However, there are several bands in the UV that arise through transitions from the 4f level to the 5d level. The 5d orbitals, unlike the 4f, are impacted by chemical interactions with surrounding atoms and ions and result in a fall in the energy of the 5d levels. Therefore, the UV absorption spectrum of cerium containing glasses is influenced by the glass composition [14]. In a silicate glass like Foturan that contains Na_2O, the Ce^{3+} absorption is an asymmetrical band with a single maximum at 314.5 nm (3.94 eV) and a FWHM of

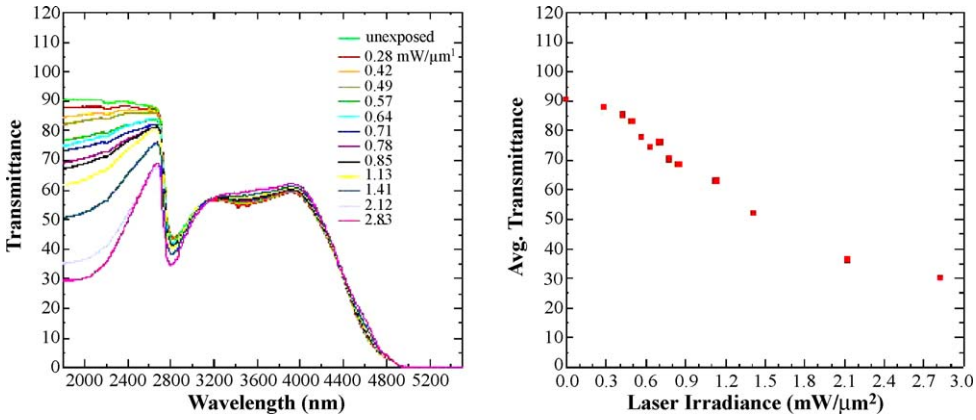

Fig. 4. Measurement of the optical transmission in the IR as a function of incident laser irradiance (λ = 355 nm) for exposed and thermally processed Foturan PSGC.

~0.5 eV [15]. Consequently, silicate-based PSGC materials that are doped with cerium are transparent in the visible wavelength region. However, Eq. (1) shows that photoexcitation process produces electrons that remain trapped in electronic defect states. These defect states have optical absorption features in the UV and the concentration of these defect states can be carefully controlled via the incident laser irradiance. Consequently, it is possible to also controllably vary the extent of absorption in the UV wavelength region as well. Control of the optical spectrum in the visible wavelength region could be accomplished by controlling the silver cluster particle size. This is the technique that is used in the development of polychromatic glass where a range of possible colors can be manufactured [16].

We have used the results shown in Figs. 2–4 to develop a variable dose laser exposure tool that uses the direct-write patterning approach to fabricate microstructures in true three-dimensions. Fig. 5 shows an example of the variable exposure dose technique as applied to the control of the local chemical solubility and the optical transmission. The optical photograph on the left shows an etched structure. A cross cut of the design profile and the actual measured depth profile are presented in the middle panel of Fig. 5, while the right panel showcases the variation of color or optical transmission in the orange-red region of the visible spectrum. In this example, the same pattern is used to showcase the ability and precision regarding control of the solubility and the optical transmission. The example also helps to illustrate the power of the variable dose approach for microstructure fabrication. Using traditional photoresist and lithographic patterning techniques (e.g., single exposure) to microfabricate the simple structure in the left panel of Fig. 5 would require four individual positive tone masks (i.e., to support the four depth levels shown) for the lithographic step alone and quite possibly another four negative tone masks to protect the complementary areas during the chemical etching phase. With variable dose and the direct-write patterning technique, no masks were used in either the patterning or in the chemical etching phase to fabricate the structure shown in Fig. 5. By controllably varying the dose during the exposure, as defined by the fit slope of the data presented in Fig. 2, *each local area etches at a different rate* so that a single timed-etch step produces all the features. Using this technique, we have patterned complex 3D structures that would normally require over 30 masks and multiple etch times if traditional lithography techniques were to be utilized (e.g., operations per masking step: apply photoresist, lithography exposure, bake, strip photoresist, and etch).

3.2. Traditional experimental setup for controlling laser irradiance during patterning

Fig. 6 shows the experimental setup used for the laser exposure and patterning studies. The pulsed UV lasers were Q-switched, diode-pumped Nd:YVO_4 systems manufactured by Spectra-Physics (OEM Models J40-BL6-266Q and J40-BL6-355Q). Typical laser pulse durations of 6.0 ± 0.5 ns (FWHM)

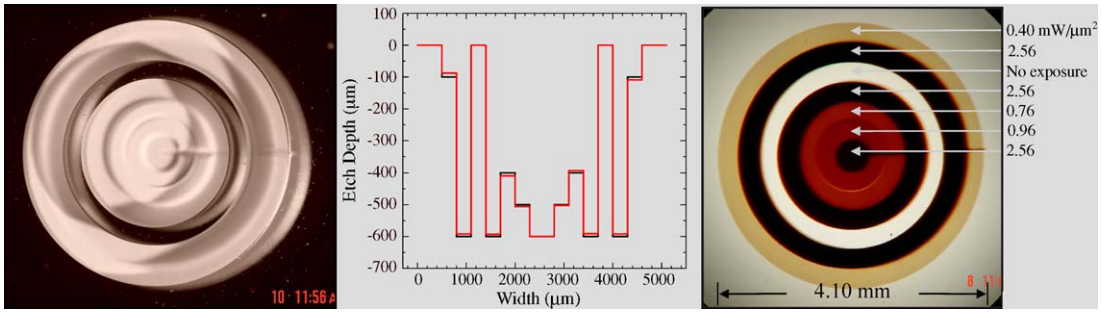

Fig. 5. Structures fabricated by the variable dose laser direct-write fabrication technique. Left: a microfabricated structure that has been chemically etched. Middle: profilometry results of the measured depth of the structure along with the design requirements. Right: the controlled local change of optical transmission in the PSGC material.

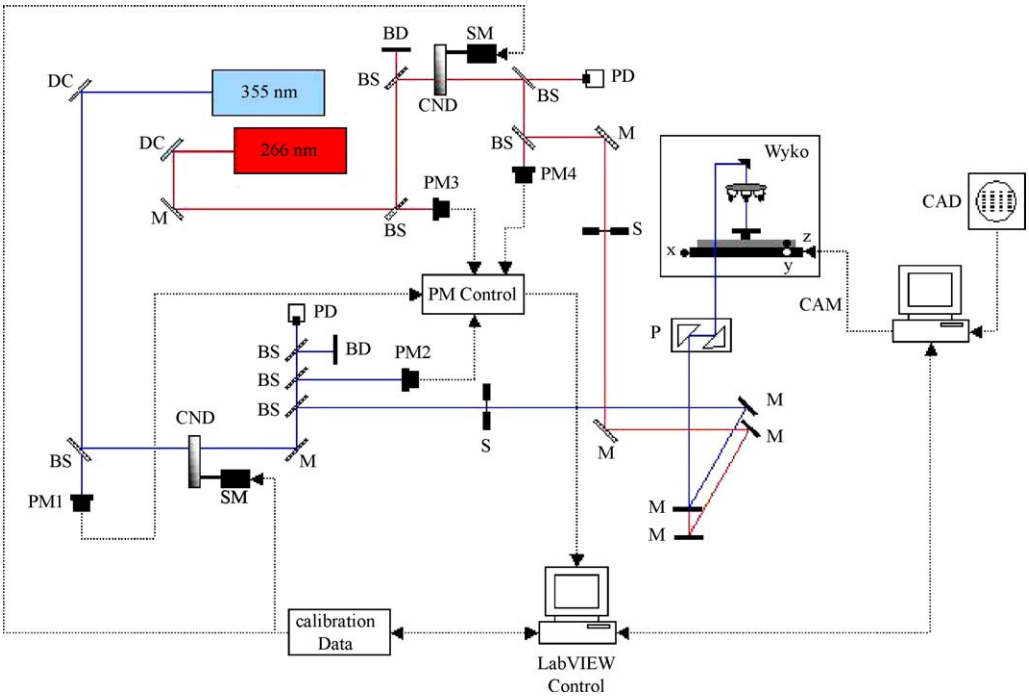

Fig. 6. Schematic representation of the experimental layout. BD, beam dump; BS, beamsplitter; CND, circular neutral density filter; DC, dichroic mirror; M, high-reflectance mirror; P, periscope assembly; PD, photodiode; PM, power meter; S, shutter; SM, stepper motor. The XYZ motion system is integrated into a non-contact, white light optical interferometer stage (WYKO/Veeco Corp.) and is controlled by computerized CADCAM software.

were achieved in the Q-switched TEM_{00} operation mode. The pulse-to-pulse stability was ±5.0% at a nominal pulse repetition rate of 10.0 kHz. The irradiation dose was applied to the glass sample using an automated direct-write, laser-patterning tool that included a circular neutral density (CND) filter (CVI Laser Corp., CNDQ-2-2.00) coupled to a micro positioning motor. A raster scan pattern was used to expose a 1.5 mm × 8.0 mm area with a laser spot diameter of 3.0 μm and a XY stage velocity of 1.0 mm/s. Over 150 samples were prepared to obtain valuable statistics. During exposure patterning, the incident laser surface power was controlled in real time by a closed-loop LabVIEW software program that monitored the power at an indicator position in the optical train. This "indicated" power could be related to the incident surface power by applying the appropriate calibration factors [17]. A UV grade, achromatic 10× microscope objective (OFR, LMU-10×-U) was used as the focusing element. For the exposure tests, several Foturan wafers (100 mm diameter, 1 mm thick) were cut into 1 cm × 1 cm square coupons and thinned to 200 and 500 μm thicknesses. The coupons were then polished to achieve an optically flat finish. The 200 and 500 μm coupons were used for the λ = 266 nm (absorptivity = 10.05/cm) and 355 nm (absorptivity = 0.27/cm) studies, respectively. The thicknesses were selected to ensure that the laser penetration depth exceeded the glass sample thickness and to minimize gradients in the exposure volume. The samples were cleaned using a RCA cleaning protocol and were subsequently handled using gloves and clean room techniques. The same cleaning technique was used for the laser microfabrication tests, except that there are multiple patterns per 100 mm diameter wafer and all patterns received the same thermal and chemical processing protocols.

3.3. High fidelity laser patterning control via digitally-scripted genotype sequence processing

Although the experimental layout schematically represented in Fig. 6 provides sufficient precision and control for fundamental investigations of the effects of laser exposure on materials, it does not provide the required precision for experiments where photoreaction control is to be integrated with complex motion patterning. The inadequacy is not because of the laser or the motion control system, but the lack of integral communication between these two systems during the patterning operations. In most laser patterning tools where direct-write techniques are employed, the motion control system utilizes a computer-assisted manufacturing (CAM) software operating system, where a motion is realized via the execution of a discrete series of commands (e.g., G-code command structures) that control the drive motors. The CAM operating system normally implements algorithms that "look-ahead" to upcoming motion sequences and adjusts motor torques accordingly to achieve the desired patterns and stage velocities. Consequently, the tangential velocity of the motion system when articulating complex motion sequences is never constant but instead is varying in preparation for the upcoming motion maneuver. The motion operating system implements these velocity modulations because it must compensate for the inertia of the stage or motion platform. As a consequence, patterned exposures, ablation, cutting, surface texturing, and other laser processing operations that utilize even the most stable laser system will be inconsistent as a direct consequence of the constantly varying velocity of the motion platform. The only types of motion that can guarantee a constant dose are raster scan motions

and these offer very limited capability for patterning complex shapes.

An ideal laser exposure patterning system would be one where each laser spot size along the direct-write pattern profile receives the same exposure dose (no. of photons/area). Better yet, each nominal spot size receives a prescribed and predefined photon dose that is designed to express a particular material functionality or property. The ideal exposure patterning system would retain two scripts. One script defines the motion control pattern in Cartesian space. This "pulse script" is assembled by using CAM and computer-assisted design (CAD) software. The second "script" includes information on the laser dose in terms of number of laser pulses and amplitudes that each laser spot size is destined to receive in Cartesian space. The second script is assembled with prior knowledge of the photochemical and photophysical properties of the photofunctional material and of the particular tool path taken during direct-write patterning. Conceptually, these two scripts are not hard to realize. The first script is CADCAM software and is commercially available, while the second is based on the results of fundamental experiments and the characterization of the photosensitive material. The missing key element is the synchronous integration of these two scripts to guarantee that every motion step on the order of the laser spot size receives the prescribed photon dose regardless of the motion control velocity.

We have developed a laser photon delivery control scheme that not only mitigates the adverse effects of velocity variation, but also allows the capability to parse the laser dose based on a predefined and prescribed need [18]. This novel laser processing technique is inspired by the genome. The genome is a sequence of concatenated genotypes that define a biological "script" of specific functional attributes that are to be expressed. In our technique, the "genotype" script is comprised of a concatenated series of amplitude-modulated voltages that drive an electro-optical (EO) Pockels cell. The inter-communication link between the laser and the motion control platform is based on a series of signal pulses generated from the motion control platform that delineates the marching of a prescribed distance along the tool path pattern. In our applications, a trigger signal is generated after moving the equivalent distance of a laser spot size in 3D Cartesian space (e.g., laser spot size with a 10× objective, 3–5 μm). The technique does not rely on the duration of time to traverse the defined distance and, as a consequence, is independent of the local velocity of the motion platform. The trigger signal drives an arbitrary waveform signal generator (AWSG), which manufactures the voltage profile that is prescribed for each specific laser spot size. The output of the AWSG is connected to the EO Pockels cell modulator. The result of synchronizing the motion platform (tool path pattern) with the amplitude-modulated laser light is that only the desired amount of light with the appropriate intensity profile is administered to each specific location. No additional light is administered until another trigger signal is received marking the transition to a new spot size. The consequence is that the motion control platform can move according to its natural inertia and the laser system can be left to run at its most effective operational mode, but the two stable systems are integrated in a common process mode that is defined by the external modulator (EO Pockels cell) and the AWSG. An appropriate analogy of this technique might correspond to a computer system, where the operating system utilizes stable clocks to create functional bytes and words that act to control a particular event. In our technique, the pulsed laser system and the motion control platform signals represent the clocks and the AWSG and the EO Pockels cell represent the operating system. We have demonstrated this technique by using an Aerotech Corp. XYZ motion stage (X; ABL80050, Y; ABL20030, Z; ALS130-150), a Tektronix Corp. AWSG (AWG 420), and an EO Pockels cell modulator system manufactured by ConOptics, Inc. We have previously shown that we can modulate a sequence of laser pulses while the motion platform is moving in excess of 400 mm/s [19].

Fig. 7 shows the technique applied to the femtosecond laser ablative scribing of Foturan glass. The results show two images that were acquired with the same optical microscope and with identical magnification and lighting conditions. The scribing pattern is an octagon structure and the magnified image is of the region near an apex where the motion velocity is expected to change. The image on the left was acquired following laser

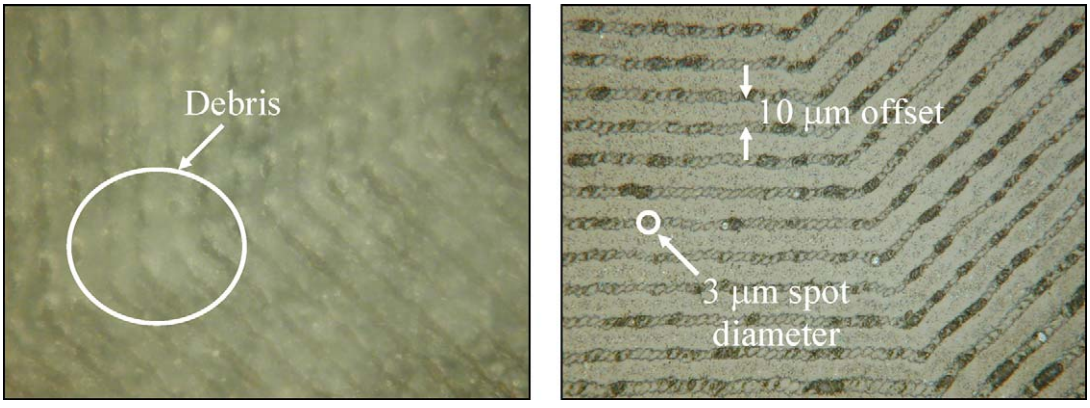

Fig. 7. Optical microscope images taken under the same microscope, magnification and lighting conditions. The images are of femtosecond laser ablative cutting of Foturan PSGC. The image on the left is without laser pulse scripting control, while the image on the right has the feature activated.

ablation without the digitally scripted genotype sequence control scheme, while the image on the right was acquired with this feature turned on. The required average power of the femtosecond laser was defined through a series of test and analysis cycles until the scribe could be judged as acceptable without the use of genotype sequence control. The laser power level was not altered for both of the cuts shown in Fig. 7. The results of this simple demonstration are compelling. The image on the left is blurred due to spallation and debris formation, while the image on the right is clear and shows highly localized material removal. We have successfully applied this technique to control the laser dose during the patterning of photosensitive materials such as Foturan, and we believe the technique is applicable to most photoreaction control experiments. Power supply drivers for Pockels cells can now be acquired with bandwidths approaching tens of MHz that facilitate light modulation with sub-100 ns transition times. For pulsed lasers operating at repetition rates of tens of MHz, the fidelity of the genotype sequence control scheme will be a strong function of the shot-to-shot power stability of the laser rather than the average power. The challenge to the laser manufacturers will be to reduce the fluctuations in the shot-to-shot peak power.

4. Conclusions

There is significant value in investigating and ultimately developing a class of "metastable" materials whose final state properties can be correlated with a set of phase transformations that are initiated by photoexcitation. Such photofunctional materials can be viewed as protean where one can assume to have the potential to transform and acquire a given set of properties from a possible multitude. Given such a protean material, a host of desirable material properties can be preferentially "switched-on" on a local scale. This is in contrast to the global transformation that is evident in traditional materials development, where the properties of the material mainly arise in accordance to the incorporated ingredients and the protocols used during manufacturing [20]. It is quite likely that such a protean material may have only a limited range of variability in the material properties, but the utility of such a material in the development of fully integrated microsystems cannot be overlooked.

Few commercially available materials purport to have protean properties. The glass ceramics are a material class that is intrinsically metastable due to the nature of the amorphous glass and the strong potential for crystallization. Combining dopants that serve as photo initiators, along with the intrinsic metastable nature of glass ceramics, results in the development of a photosensitive glass ceramic that can then be locally altered in 3D space using pulsed lasers. Furthermore, the utilization of lasers to control the exposure and thereby establish conditions to drive a particular phase transformation path allows for the unique property of lasers (i.e., variability of wavelength, frequency, resonant, or non-resonant (heating)) to "produce" a unique material with a mosaic of specific material phase distributions. We have initiated an experimental program to investigate the use of laser excitation in defining initial state conditions in a commercially available PSGC and to evaluate the subsequent effect on the final state material properties. Without the ability to alter the material ingredients, we have been able to control the chemical solubility, optical transparency, and over a limited range the hardness (modulus of rupture) of the final state material. Our results have provided sufficient confidence to argue that other protean materials can and should be developed. Consequently, we have also seen the need for an enhanced means of optical control during photon exposure patterning. Specifically, there is a need to merge information about the pattern that represents the desired property changes with the means that control the photolytic source to selectively initiate the requisite photoreaction process. In the latter regard, we have developed an approach that is inspired by the genome and the functional operative represented by the genotype.

Acknowledgements

The authors thank the Aerospace-sponsored Independent Research and Development Program (IR & D) and the Air Force Office of Scientific Research (AFOSR, Dr. H. Schlossberg, Program Manager) for their generous financial support. We also wish to thank Mr. Paul Adams of the Materials Processing & Evaluation Department for assistance in the optical spectroscopy measurements.

References

[1] W. Holand, G.H. Beall, Glass-Ceramic Technology, The American Ceramic Society Press, Westerville, OH, 2002.
[2] H. Helvajian, 3D microengineering via laser direct-write processing approaches, in: Direct-Write Technologies for Rapid Prototyping Applications, Academic Press, New York, 2002, p. 415.
[3] F.E. Livingston, H. Helvajian, Photophysical processes that lead to ablation-free microfabrication in glass-ceramic materials, in: H. Misawa, S. Juodkazis (Eds.), 3D Laser Microfabrication, Wiley–VCH Verlag GMBH & Co., Weinheim, Germany, 2006, p. 287.
[4] S. Janson, A. Huang, W. Hansen, H. Helvajian, Development of an inspector satellite propulsion module using photostructurable glass/ceramic materials, J. AIAA (2004) 6701.
[5] A. Berezhnoi, Glass-Ceramics and Photo-Sitalls, Plenum, New York, 1970.
[6] S.D. Stookey, Chemical machining of photosensitive glass, Ind. Chem. Eng. 45 (1953) 115.
[7] F.E. Livingston, H. Helvajian, Appl. Phys. A 81 (2005) 1569.
[8] Foturan Specification Information Guide, Schott Corporation Technical Glass Division literature F10/1999.
[9] F.E. Livingston, P.M. Adams, H. Helvajian, J. Appl. Phys., in press.
[10] F.E. Livingston, P.M. Adams, H. Helvajian, Appl. Surf. Sci. 247 (2005) 526.
[11] U. Kreibig, Appl. Phys. 10 (1976) 255.
[12] J. Bosbach, C. Hendrich, F. Stietz, T.A. Vartanyan, T. Wenzel, F. Traeger, Laser manipulation of the size and shape of supported metal nanoparticles, in: Proceedings of SPIE, vol. 4274, 2001, p. 1.
[13] R. Reisfeld, Spectra and energy transfer of rare earths in inorganic glasses, in: J.D. Dunitz, P. Hemmerich, J.A. Ibers, C.K. Jorgensen, J.B. Neilands, R.S. Nyholm, D. Reinen, J.P. Williams (Eds.), Structure and Bonding, vol. 13, Spring-Verlag, New York, 1973, p. 53.
[14] J.A. Duffy, G.O. Kyd, Ultraviolet absorption and fluorescence spectra of cerium and the effect of glass composition, Phys. Chem. Glasses 37 (1996) 45.
[15] J.S. Stroud, Photoionization of Ce^{3+} in glass, J. Chem. Phys. 35 (1961) 844.
[16] S.D. Stookey, G.H. Beall, J.E. Pierson, J. Appl. Phys. 49 (1978) 5114.

[17] F.E. Livingston, H. Helvajian, Proceedings of SPIE, vol. 4830, 2003, p. 189.
[18] F.E. Livingston, H. Helvajian, On-line Proceedings of the 6th International Symposium on Laser Precision Microfabrication (LPM), 2005.
[19] F.E. Livingston, H. Helvajian, Laser Material Processing Inspired by Digitally-Scripted Genotype Sequencing, U.S. Patent filed under Docket No. D-526 (2004).
[20] P.L. Higby, J.E. Shelby, Properties of some simple glass/ceramic systems, J. Am. Ceram. Soc. 67 (1984) 445.